

Heat transfer in laminar, oscillatory flow in cylindrical and conical tubes

ROBERT A. PEATTIE

Department of Chemical Engineering, Johns Hopkins University, 34th and Charles St., Baltimore, MD 21218, U.S.A.

and

RALPH BUDWIG

Department of Mechanical Engineering, University of Idaho, Moscow, ID 83843, U.S.A.

(Received 4 April 1988 and in final form 6 October 1988)

Abstract—In order to assess the effect of frequency on transport of a passive scalar contaminant in an oscillatory flow, a piston-driven pipe flow is established. Two pipe test section geometries are used: one straight, round, and uniform and the other uniformly tapering (i.e. conical). Flow is driven at frequencies characteristic of human breathing, both resting, normal and high frequency. A screen of closely spaced, parallel, thin wires is placed perpendicular to the flow, in the test section, and is heated so as to dissipate a constant power into the fluid. The subsequent time-average and instantaneous temperature fields are measured, as functions of position. The results are shown to be consistent with the consequences of transport of heat by a combination of convection and diffusion. Convective transport is found to increase with frequency, at constant amplitude, but the effective diffusivity does not obey the predictions of theories which are based on an assumption of constant average axial gradient of the scalar field.

1. INTRODUCTION

RECENTLY it has been clearly demonstrated by a number of authors (e.g. Lunkenheimer *et al.* [1], Bohn *et al.* [2], and Slutsky *et al.* [3]) that human respiration can be driven artificially at volumes significantly less than normal resting breathing volumes if frequencies greater than resting breathing frequencies are used. Inasmuch as traditional physiological ideas forbid gas exchange when breathing volumes are smaller than a fixed minimum called the respiratory dead space, a limit which is routinely violated during high frequency ventilation (HFV), interest has been sparked in the mechanism by which gases are transported through the lung during breathing.

Little is yet known about the details of the velocity and concentration fields within the respiratory system, principally because the pulmonary anatomy consists in large part of a complex three-dimensional series of branching tubes, which lead to secondary swirling flow patterns and in some areas turbulence. Investigators wishing to gain insight into transport mechanics have therefore resorted to simplified geometries, of which the most obvious is the straight tube.

Taylor [4] showed that for a diffusing mass species in a rigid pipe if (i) the flow is steady, (ii) the axial molecular diffusion is negligible compared to the axial convective transport, and (iii) the time scale for radial molecular diffusion is much less than the time scale for axial convection, then the effects of longitudinal convection and radial diffusion can be combined into

one effective parameter which he called the virtual coefficient of diffusion, D_{vir} , for the species. For a circular tube he found

$$D_{\text{vir}} = \frac{a^2 \langle U \rangle^2}{48 D_{\text{mol}}} \quad (1)$$

where a is the pipe radius, $\langle U \rangle$ the area averaged velocity, and D_{mol} the molecular diffusion coefficient. Physically, Taylor suggested that the spreading of solute in the pipe, from some initial distribution, is governed by a combination of convective and diffusive motions. Axial transport is greater than would be expected on the basis of molecular diffusion alone, approaching that rate in the limit of low velocity or high molecular diffusivity. On the other hand radial molecular diffusion reduces the streamwise transport from what it would be for a non-diffusing species, because of material exchange between the rapidly moving center of the flow and the slowly moving area near the wall. The type of transport which arises from these effects is commonly referred to as augmented diffusion.

It can be shown (see Aris [5]) that if restrictions (ii) and (iii) are removed, the effective diffusion coefficient, D , is given by

$$D = D_{\text{mol}} + D_{\text{vir}} \quad (2)$$

Mass dispersion in purely sinusoidal flows in straight tubes has been studied by Chatwin [6], Watson [7], and Joshi *et al.* [8], among others. For

NOMENCLATURE

a	pipe radius	V	control volume
A	flow amplitude	x	axial coordinate.
C_v	fluid specific heat, at constant volume	Greek symbols	
d	pipe diameter	α	Womersley number
D	effective diffusion coefficient of a material solute	$\theta(r, \phi, x, t)$	instantaneous temperature
D_{mol}	molecular diffusion coefficient	κ	fluid thermal diffusivity
D_{vir}	virtual diffusion coefficient	K_{eff}	effective thermal diffusivity
k	fluid thermal conductivity	ν	fluid kinematic viscosity
P	power dissipation of source	ρ	fluid density
Q_{conv}	convective energy transfer in one cycle	σ	Schmidt number
r	radial coordinate	τ	flow period
S	control volume boundary	ϕ	azimuthal coordinate
$T(r, \phi, x, t)$	temperature	ω	flow angular frequency.
T_{amb}	ambient temperature	Other symbols	
$u(r, \phi, x, t)$	instantaneous velocity	$\langle \quad \rangle$	average with respect to area
$U(r, \phi, x, t)$	velocity	$\bar{\quad}$	average with respect to time.

such harmonic flows, although the same basic mechanism applies as governs the steady flow case, the qualitative nature of the results is quite different. To begin with, in the absence of diffusion, under laminar conditions net transfer of material can no longer occur, since fluid returns to its initial position after any integral number of cycles. Even if diffusion is allowed, however, there may still be little augmentation of transport if the transverse mixing time scale is short compared to the period of the flow. Nevertheless, for times long compared with the time scale of transverse diffusion, under the assumption that the time-averaged concentration field has a constant axial gradient, Chatwin [6] has shown that the dispersion is augmented, and by terms the frequency of which is twice the oscillation frequency. Under these conditions, the time-average effective diffusion coefficient reduces to equation (2). Watson [7], likewise assuming a concentration field the time average of which is linear in the longitudinal coordinate, provided an explicit solution for the field profiles as a function of position and time. Then by integrating over a cross-section he found

$$D = D_{\text{mol}}(1 + R) \quad (3)$$

with

$$R = f_s(\alpha^2, \sigma) \left(\frac{2A}{a} \right)^2 \quad (4)$$

A is the flow amplitude, α the Womersley number ($= a(\omega/\nu)^{0.5}$ with ω the flow angular frequency and ν the fluid kinematic viscosity) and σ the Schmidt number ($= \nu/D_{\text{mol}}$). The function f_s depends also on the shape of the pipe. Watson was able to evaluate the material flux for arbitrary frequency for a circular

pipe and a two-dimensional channel, and was able to study the flux for any cross-sectional shape in the limiting cases of low and high flow frequency. Unfortunately, no experiment yet has examined these theoretically predicted concentration profiles.

The analogous problem with heat as the contaminant has been analyzed by Kurzweg and de Zhao [9–11]. Among the special cases in this work is included one corresponding to mass dispersion, with the radial temperature gradient at the pipe wall taken as zero, which is equivalent to a supposition of perfectly insulated walls. In practice experiments with a material solute or heat both are subject to trade-offs. No method has been developed which allows mass concentration to be measured with the spatial and temporal resolution necessary for establishment of relevant concentration fields, which vary in both space and time. In contrast, temperature fields can be determined with very small probe length scales (< 0.1 cm) and very fast time response (> 1 kHz), but in a heat transfer experiment the normal temperature gradient at the wall can only approximately be reduced to zero.

The purpose of this paper is to study, in detail, the temperature field and thermal transport properties of laminar oscillatory flows in two simple geometries which are relevant to pulmonary ventilation. Shapes chosen are the straight round tube of uniform cross-section and the linearly tapered round tube. A range of dimensionless frequencies is covered which is characteristic of HFV. For experimental simplicity, and for ease of control, a constant low power plane heat source is used to produce purely passive thermal contamination of the flow. Time and area averaged quantities, including the thermal equivalent of D , are calculated from instantaneous point measurements of temperature.

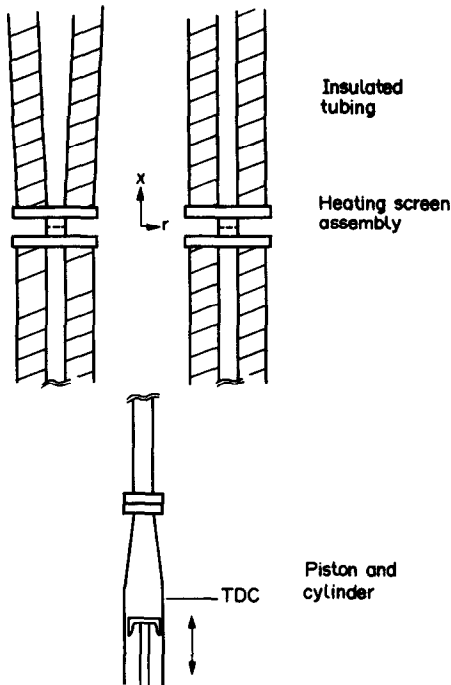


FIG. 1. Schematic diagram of the flow apparatus, showing both test sections.

2. METHODS

Figure 1 shows the oscillating flow apparatus. The working fluid, air, was driven by a piston, which in turn was driven by a variable speed d.c. motor through a scotch yoke. Since the amplitude of piston motion was adjustable, the amplitude and frequency of the flow could be independently set. An optical encoder mounted on the end of the yoke flywheel shaft produced two output wave trains, which were used to monitor the flow period and to provide a timing signal, referred to piston top dead center, from which phase related information could be derived.

The piston cylinder was joined by a 20 cm long tapered tube to a 2.5 cm diameter tube which ran 100 cm to the test section. Two test sections were used in these experiments: one had a uniform cross-section 2.5 cm in diameter and a length of 25 cm, while the other was conical with a 4° total included angle and a length of 60 cm. To minimize end effects, straight tubing was continued for more than 150 cm beyond the end of the uniform test section, and for more than 50 cm beyond the conical section. In each case the tube was open at its end to ambient air. The whole apparatus was oriented along a vertical axis. Flow amplitudes from 7 to 11 cm were used (for the conical tube, amplitudes and dimensionless frequencies refer to the base of the cone). Consequently the flow was always laminar, as is discussed in ref. [12].

A biplanar mesh heat source was inserted in the flow. The source consisted of two planes of parallel

0.0025 cm diameter nichrome wires, with the upper plane strung perpendicularly to the lower and separated from it by 0.32 cm. The screen mesh length was 0.21 cm, and the solidity was 2.3%. For convenience of operation the screen was positioned at the top of the uniform test section, and so was distal to the piston, but was placed at the base of the cone. Thus it was proximal to the piston for the latter case. However, the source was powered by a d.c. voltage supply, which was adjusted to just produce the greatest thermal dissipation from which no buoyancy driven velocity could be measured, so that temperature records were symmetric about the screen. A constant power, P , of 1/4 W was dissipated by the screen into the tube. Closed cell foam insulation was placed around the tube for 50 cm on either side of the heating screen, and a series of holes was bored through the insulation and tubing wall to allow for the passage of probes.

During all experiments, the room air was mixed by a vertically oriented blower to ensure a uniform mean temperature around the apparatus.

Time-averaged temperatures were measured with a thermistor (Fenwal Electronics GB41J1) mounted on a cylindrical probe. When the thermistor was extended to the centerline of the uniform cross-section tube, the probe occupied 0.4% of the cross-sectional area of the tube. To generate a difference signal, a second thermistor was positioned outside the insulated wall of the test section. Both thermistors were calibrated against a reference thermometer in a jet of heated air; the standard deviation of a typical calibration was 0.03°C . The two thermistors were connected to a circuit which gave voltage outputs proportional to the temperatures, and whose sensitivity was linear over the range of temperatures measured (see ref. [12] for details).

Instantaneous temperature profiles were measured with a platinum wire resistance thermometer etched to 0.0001 cm diameter and 0.06 cm length, and mounted on a similar cylindrical probe. The wire was provided with an operating current of 0.5 mA through a circuit which also delivered a voltage output proportional to the wire resistance. (This circuit is fully described in Peattie [13]; it is shown that a noise limited resolution of less than 0.01°C is achieved.) The -3 dB point in the frequency response of such wires has been estimated by LaRue *et al.* [14] and Hojstrup *et al.* [15] to occur at about 3 kHz. Records of the wire voltage taken in unheated flow were used to correct for the small spurious velocity sensitivity of the wire.

Since the thermistor circuit outputs were steady, they were read directly on a voltmeter. The wire circuit outputs, however, were amplified with a Tektronix AM502 differential amplifier, low-pass filtered, digitized on a Data Translation DT2801-A A/D converter, and stored on an IBM Personal Computer, and then were ensemble averaged with from 20 to 150 realizations, depending on flow frequency.

3. RESULTS

Cylindrical polar coordinates (r, ϕ, x) are taken with origin on the tube centerline, midway between the two heating screen planes (as shown in Fig. 1). Measurements were taken only after the time-mean temperature field had asymptotically reached a steady state. Hence the temperature at any point in the flow can be written as the sum of a steady term and a term fluctuating periodically in time. Further, since the geometry of the experiment is axisymmetric (except for the presence of the probe) we have

$$T(r, x, t) = \bar{T}(r, x) + \theta(r, x, t) \quad (5)$$

where t indicates time, and the overbar denotes an average with respect to time.

Figure 2 shows periodic temperature fluctuations

on the centerline of the uniform cross-section tube, for four axial positions. Figures 2(a)–(c) differ in flow frequencies, being data for $\alpha = 5.7, 16$, and 20 , respectively. The duty cycle of the temperature fluctuation decreases with distance from the heating screen in all cases. The amplitude of the temperature excursion, however, increases with distance from the screen, or remains approximately constant, for distances up to two flow amplitudes, then decreases rapidly for larger distances. Moreover, for the two high frequency cases θ is roughly symmetric from one half cycle to the next, while for $\alpha = 5.7$ the sharp temperature peaks which occur in the first half cycle are not repeated during the second half cycle.

These periodic temperature fluctuations in the tube core are consistent with the effects of a warm slug of

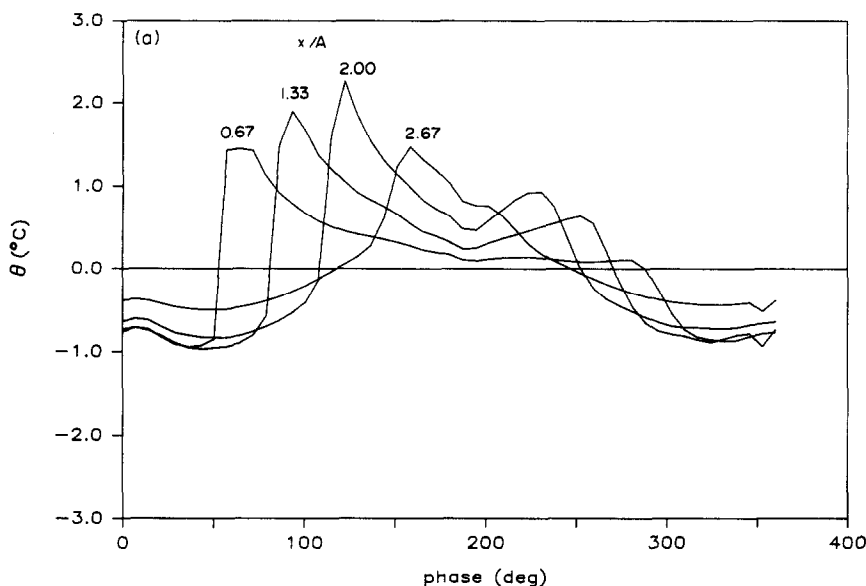


FIG. 2(a). Instantaneous temperature on the centerline of the uniform tube, for $\alpha = 5.7$.

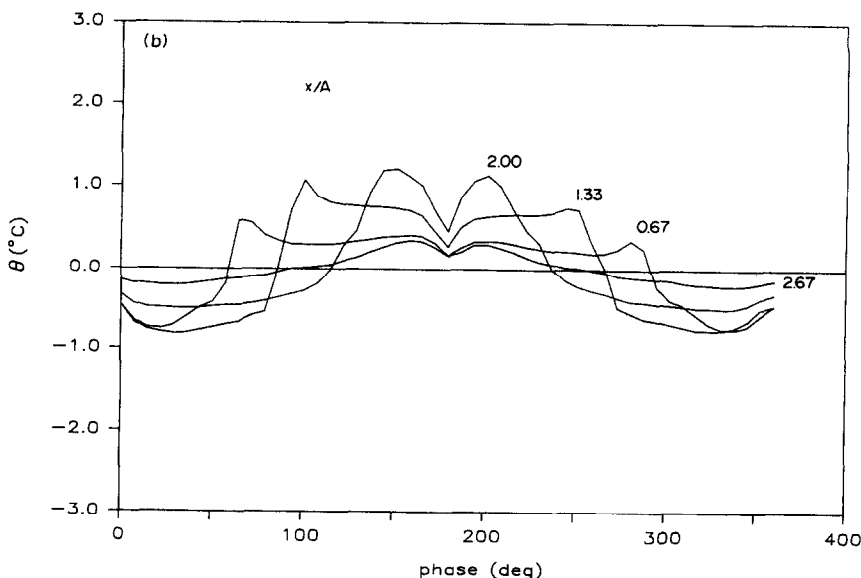


FIG. 2(b). Instantaneous temperature on the centerline of the uniform tube, for $\alpha = 16$.

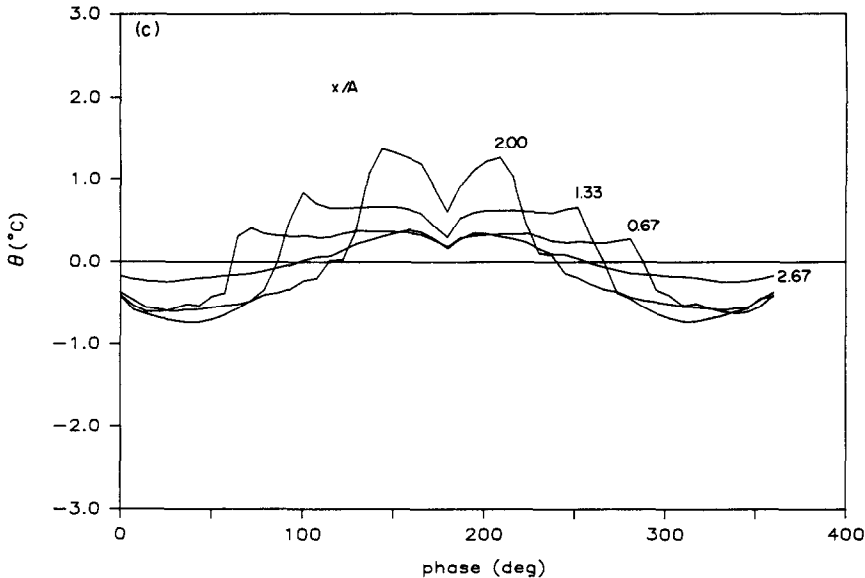


FIG. 2(c). Instantaneous temperature on the centerline of the uniform tube, for $\alpha = 20$.

air moving back and forth, with a peak travel of roughly two amplitudes from the screen. As a result of constant power injection into the flow, the extent to which air within the slug is heated depends on its velocity as it passes the screen. In support of this idea is the fact that the temperature peak in Fig. 2(a) is considerably larger than those in Figs. 2(b) and (c). Also, as frequency increases, less heat diffuses radially away from the centerline in a half cycle. Therefore, at $\alpha = 16$ and 20, fluid at a given temperature passing the probe during one half cycle returns past the probe at nearly the same temperature during the next half cycle, so that these curves are symmetric. In contrast, at low frequency, fluid passing the probe during the first half cycle has given up heat, and cooled down, before returning past the probe in the second half cycle.

Two reasons may be given for this behavior. First, as frequency decreases, there is more time in which radial diffusion can act. Second, at $\alpha = 5.7$, the velocity profile is nearly parabolic. As a result, the centerline fluid, although not warmed as much in passing the screen as the fluid near the wall, travels further downstream in a half cycle than the fluid which surrounds it. Thus an instantaneous radial gradient is set up at the centerline, which leads to the removal of heat from the fluid at the centerline. In contrast, at $\alpha = 16$ and 20 the velocity profile is flat in the core region. Therefore, no radial gradient, or at least a much weaker gradient, is expected.

Periodic temperature fluctuations on the centerline of the tapered tube, which are not presented here, were found to be qualitatively similar to the results shown in Fig. 2.

Figure 3 gives data for the mean temperature field, $\bar{T}(r, x)$ (minus the ambient temperature) for the uniform cross-section tube. Again Fig. 3(a) shows the case $\alpha = 5.7$, while Figs. 3(b) and (c) are for $\alpha = 16$

and 20. In each experiment $\partial \bar{T} / \partial r < 0$ for r off the centerline, including for $r/a = 0.9$, which indicates that even in the mean some heat is lost through the tube walls, in spite of the insulation. However, the low frequency case has a core flow temperature profile which is much more nearly flat than the high frequency cases. In addition the magnitude of the axial temperature gradient at $\alpha = 5.7$ is less than at higher frequencies, for all radii.

Figure 4 shows $\bar{T}(r, x)$ (again, minus the ambient) for the 4° tube. These results differ qualitatively from $\bar{T}(r, x)$ for the uniform tube, which is clearly the result of essential differences in the nature of the flow, caused by the axially asymmetric geometry. Grotberg [16] has shown theoretically, and ref. [12] has confirmed experimentally, that in the presence of linearly diverging tube walls the time averaged velocity at any point is not, in general, zero. Rather concentric rings of fluid are set up which drift, in the mean, towards one or the other end of the tube. The number of such annuli and the location of their radial boundaries are functions of α . As shown in Fig. 4(b), $\alpha = 16$ radial mean temperature profiles have a positive slope in the core region, a maximum at roughly $r/a = 0.5$, and then a negative slope in the annulus adjacent to the wall. In contrast the $\alpha = 16$ straight tube experiment (Fig. 3(b)) has a negative slope for all radii. The same comment applies for $\alpha = 20$, except that here the maximum in \bar{T} occurs more nearly at $r/a = 0.7$. These results correspond very strongly with drift velocity profiles given previously. At $\alpha = 20$ there are three zones in the flow: a core of fluid moving towards the narrow end of the tube (which in the present experiment would convect cool air from the wide end of the tube), surrounded by a region drifting towards the wide end the peak velocity of which is at about $r/a = 0.75$ (this would draw warm air here), and

finally a thin layer near the wall directed towards the narrow end.

At $\alpha = 5.7$ the same general physics applies, but the greatest mean temperature occurs now at r/a of only about 0.2. This inward displacement of the peak would be consistent with either a three area drift profile with two very narrow inner zones and one wide outer zone, or with a two region profile in which the inner region is moving towards the wider end with a maximum velocity at $r/a = 0.2$. No velocity measurements exist to distinguish between the possibilities.

Isotherms of θ for the uniform cross-section tube at $\alpha = 16$ are shown in Fig. 5. It should be noted that the aspect ratio given by the figure does not match that of the actual test section, which tends to make

the radial temperature gradients appear smaller than they in fact are. Were the temperature field fully axisymmetric, the slope of all isotherms would be zero at the centerline. Many of the curves, however, have non-zero slopes at $r = 0$, an indication of asymmetry which is presumably due to withdrawal of heat from the tube by the metallic probe body, and the aluminum bushing which supports it.

Some of the isotherms for the $\alpha = 5.7$ case are closed curves, as shown in Fig. 6 (only half the tube is shown), which implies the existence of pockets of warm air in the flow. By calculating the transit time of fluid in the core of the tube, it can be shown that these are formed from air that was at the screen when the flow was temporarily stagnant.

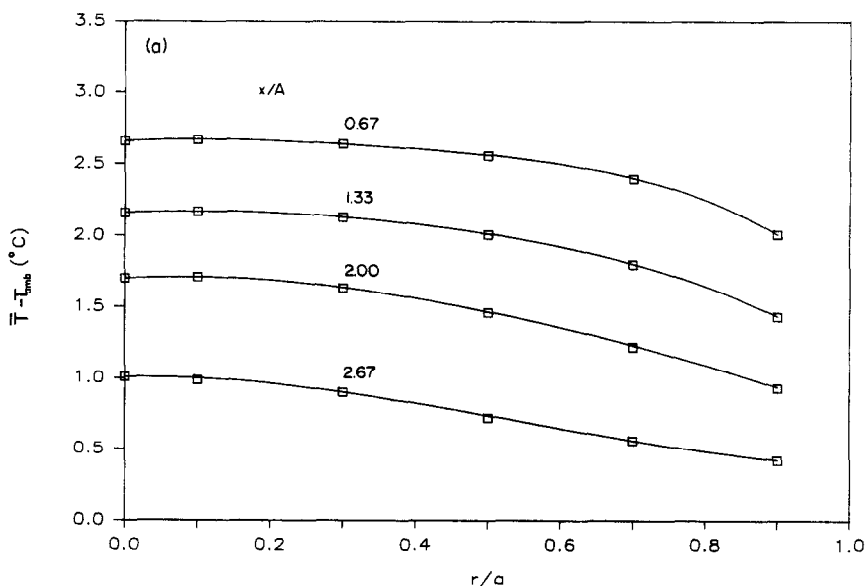


FIG. 3(a). Mean temperature field in the uniform tube, $\alpha = 5.7$.

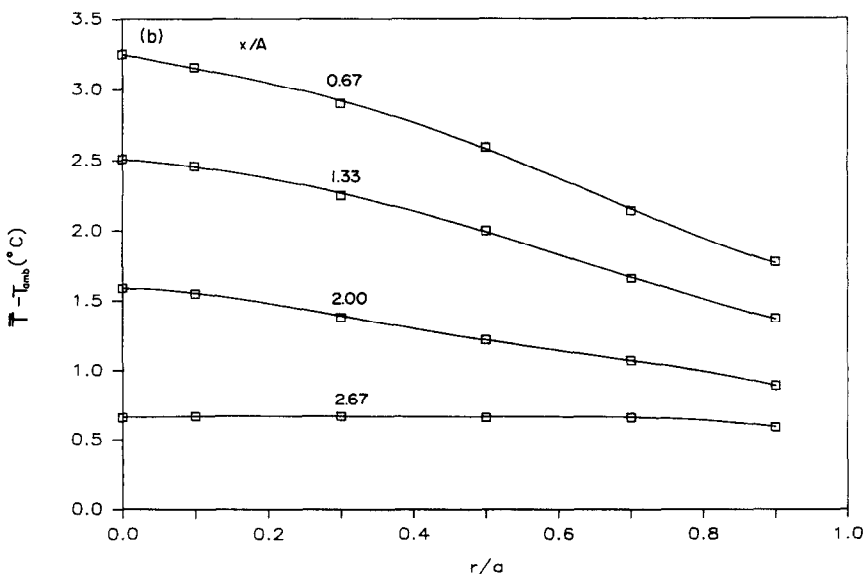
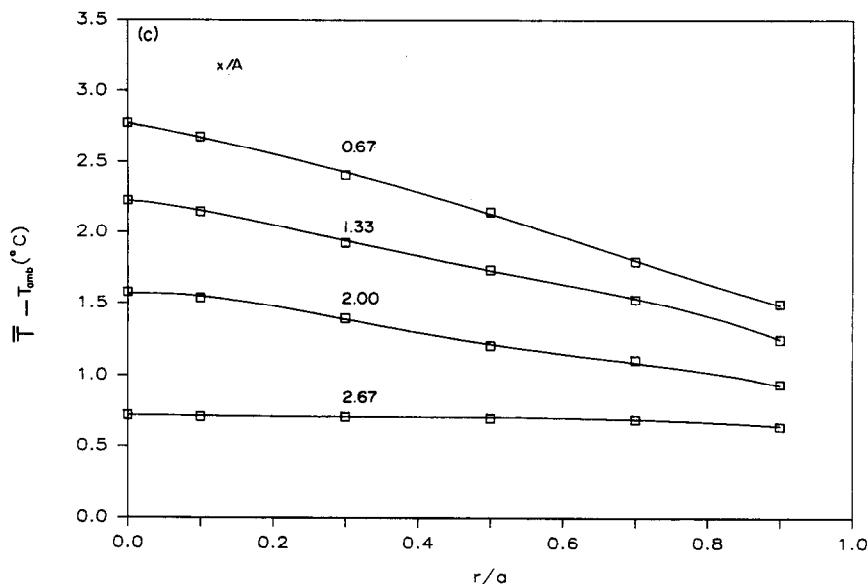


FIG. 3(b). Mean temperature field in the uniform tube, $\alpha = 16$.

FIG. 3(c). Mean temperature field in the uniform tube, $\alpha = 20$.

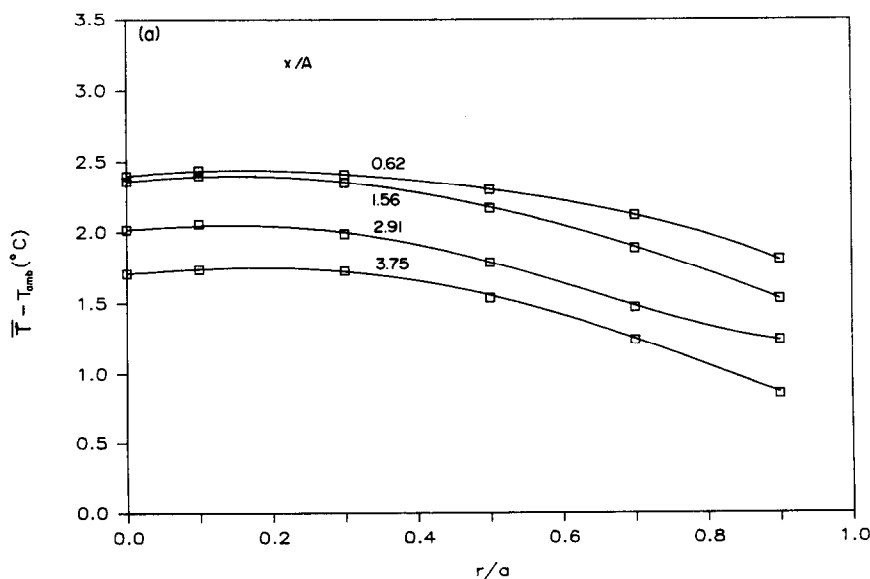
The radial gradients, $\partial\theta/\partial r$, seen in Figs. 5 and 6 point out that a Taylor-type augmentation is in effect in this flow. When the flow is in one direction, a core of warm air travels down the tube and sets up a large $\partial\theta/\partial r$, resulting in radial transfer of heat into the boundary layer. When the flow reverses, the warmed boundary layer does not convect the heat back as the core flow would have. Over many cycles the transport of heat down the tube is greatly enhanced by the flow, even though the fluid shows no net motion. In addition, $\partial\theta/\partial r$ does not appear to approach zero at $r = a$. Therefore, heat is being passed to, and regeneratively received from, the tube walls. This effect might be analogous with the transfer of oxygen and carbon dioxide to and from moist airway walls.

4. DISCUSSION

To interpret these results, a section of the tube may be taken as a control volume. If the volume is chosen so as not to include the source, for simplicity, and if gravitational potential energy and viscous dissipation are ignored, then the balance of energy of the volume is expressed by

$$\rho C_v \left[\int_V \frac{\partial T}{\partial t} dV + \int_S T \mathbf{U} \cdot d\mathbf{S} \right] = k \int_S \nabla T \cdot d\mathbf{S} \quad (6)$$

where ρ is the fluid density, C_v its specific heat, k its thermal conductivity (all assumed constant), V the control volume, and S its boundary. Since, from equation (5), T is the sum of a mean and a periodic fluctuation,

FIG. 4(a). Mean temperature field in the conical tube, $\alpha = 5.7$.

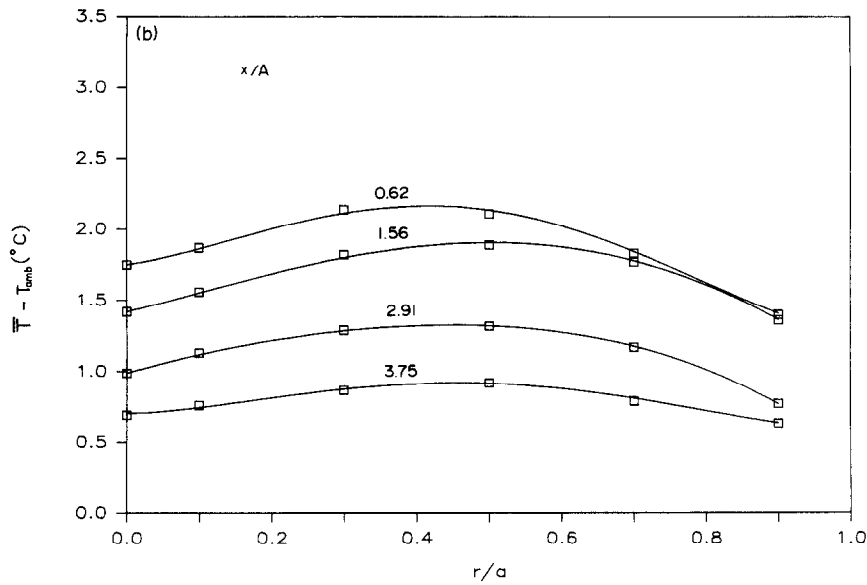


FIG. 4(b). Mean temperature field in the conical tube, $\alpha = 16$.

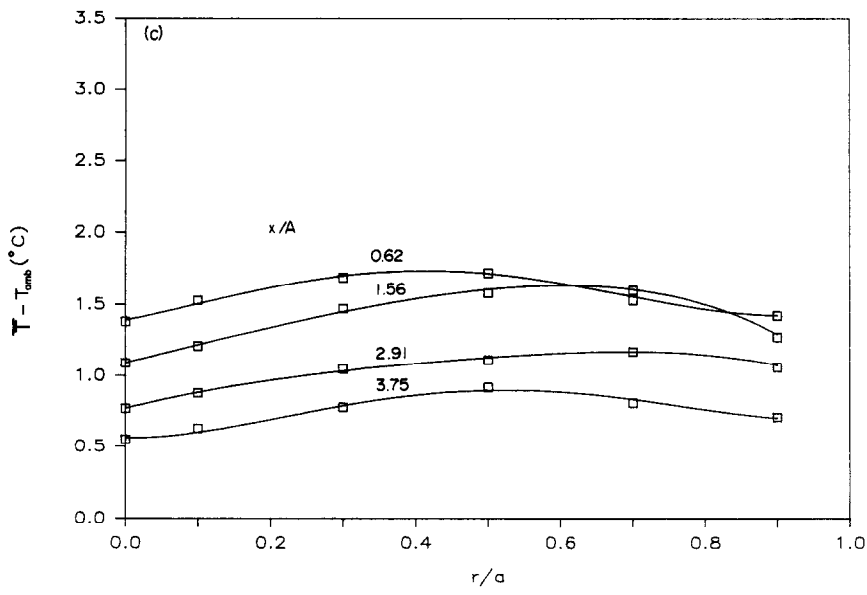


FIG. 4(c). Mean temperature field in the conical tube, $\alpha = 20$.

tuation, the unsteady term can be removed from equation (6) by integrating over a period. Denoting the period by τ , this leaves

$$\rho C_v \int_0^\tau \int_S \mathbf{TU} \cdot d\mathbf{S} dt = k \int_0^\tau \int_S \nabla T \cdot d\mathbf{S} dt. \quad (7)$$

Physically, therefore, once the system has reached a stationary state, over a cycle the net energy transfer into V by convection is balanced by that transferred by conduction.

Estimating from the data of Figs. 3 and 4, less than 1% of axial energy transfer is by conduction. Hence, axial transport occurs essentially by convection. Conversely, radial transport through the wall is due only to conduction. Transport through the wall is not

solely a mechanism for heat loss, however, as it has been shown in Figs. 5 and 6 that heat is both transferred to and received from the wall.

Let the energy transferred through any plane $x = \text{const.}$ over a single period, by convection, be Q_{conv} . The velocity field is given by a mean term $\bar{U}(r, x)$ plus a periodic term $u(r, x, t)$. Thus

$$Q_{\text{conv}} = 2\pi\rho C_v \int_0^\tau \int_0^a (\bar{T}\bar{U} + \theta u) r dr dt. \quad (8)$$

If the tube is uniform, $\bar{U} = 0$. Figure 7 shows Q_{conv} for the uniform section, evaluated with an analytical solution for $u(r, t)$ (see, e.g. Gerrard [17]) and empirical results for $\theta(r, x, t)$, as a function of axial distance from the screen, for two dimensionless frequencies,

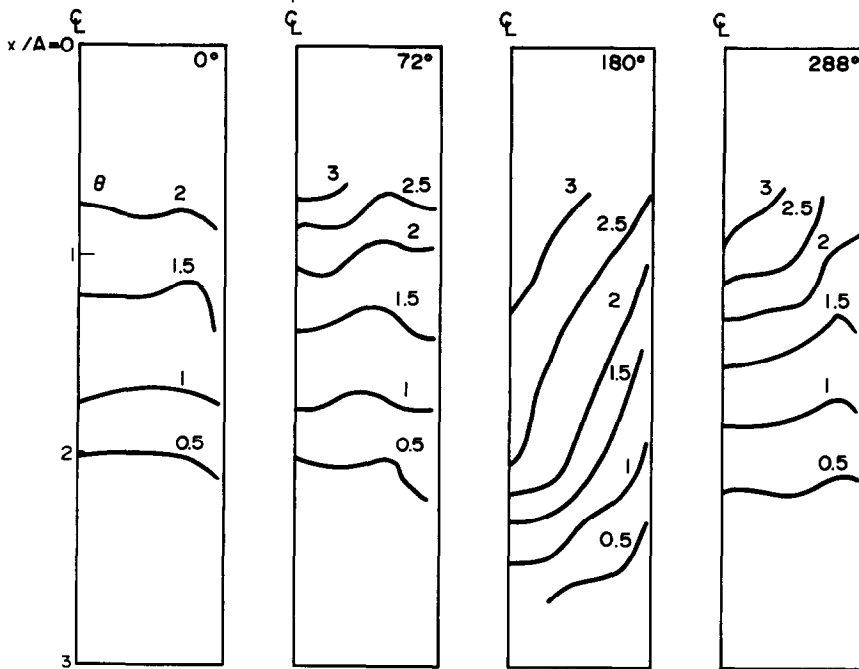


FIG. 5. Isotherms of θ for the uniform tube, with $\alpha = 16$, at four phases of the flow: 0° , 72° , 180° , and 288° (after top dead center).

with $A/d = 3$ (where d is the tube diameter). The results have been normalized by one half the energy delivered by the screen in one period. Two points are clear. First, since there is a net heat loss through the tube walls, Q_{conv} decreases as x increases. Second, convective energy transfer per cycle increases with frequency, at least in the range $5 \leq \alpha \leq 16$. Q_{conv} at

$\alpha = 16$ is from 65 to 100% greater than at $\alpha = 5.7$, depending on position.

Also shown are three points taken from the conical section, with $A/d = 4$ and $\alpha = 16$. At the measuring stations this produced (i) $A/d = 2.88$ and $\alpha = 18$, (ii) $A/d = 1.73$ and $\alpha = 21$, and (iii) $A/d = 1.28$ and $\alpha = 24.5$. Although α is proportional to the tube

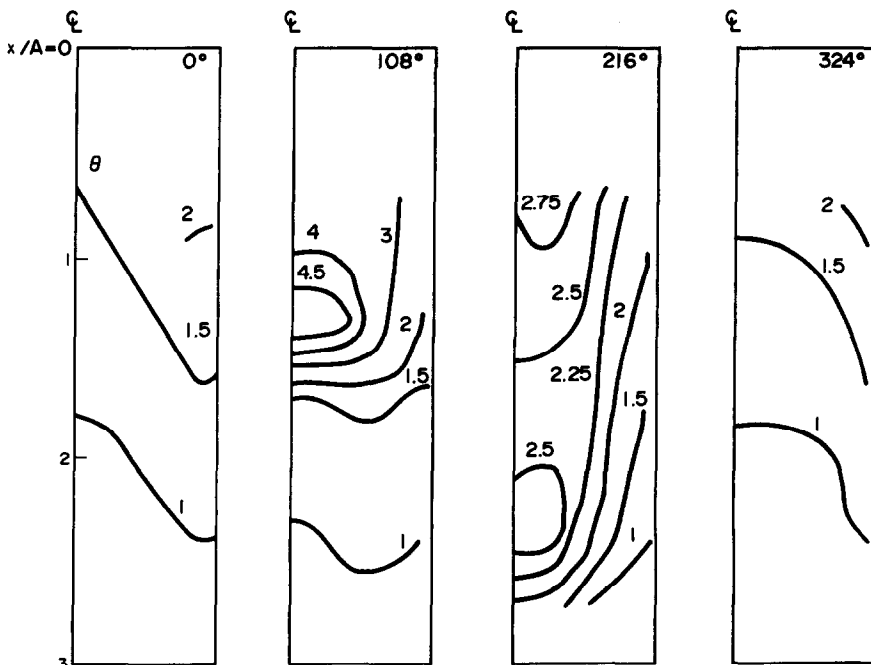


FIG. 6. Isotherms of θ for the uniform tube, with $\alpha = 5.7$, at four phases of the flow: 0° , 108° , 216° , and 324° (after top dead center).

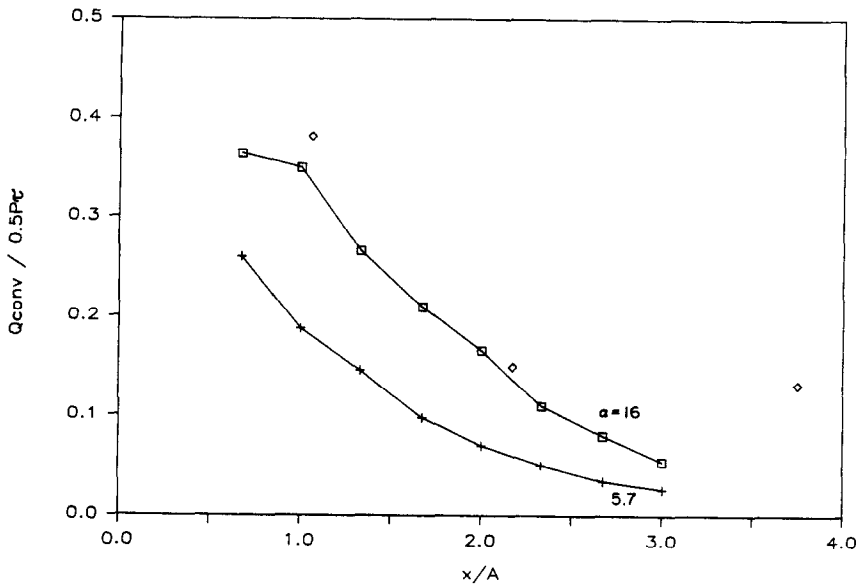


FIG. 7. Q_{conv} for the uniform tube, with $A/d = 3$, and three points from the conical tube, as described in the text.

radius, the transport of energy does not increase with x . Rather the flow amplitude decreases with a^2 , from conservation of mass, which results in Q_{conv} falling monotonically with x , as seen.

Neglecting the negligible contribution of conduction to the axial transport, the effective mean axial diffusivity for thermal energy transfer in a tube, K_{eff} , is given by

$$K_{\text{eff}} = \frac{Q_{\text{conv}}}{\pi a^2 \rho C_p \tau \frac{d\langle T \rangle}{dx}} \tag{9}$$

The results for K_{eff} , normalized by the thermal diffusivity, κ , are shown in Fig. 8. Figure 8(a) shows the

case $A/d = 3$ from the uniform tube, for two frequencies, along with corresponding results from Watson [7], which are independent of position. Figure 8(b) shows K_{eff} for $A/d = 4$, with additional values from Watson [7], and also shows three points from the conical test section, the frequencies and amplitudes of which were specified above. In the present experiment, K_{eff} increases by a factor of from two to three as A goes from three to four d , for $\alpha = 5.7$, but hardly increases at all with A/d for $\alpha = 16$. Nevertheless, the rise of K_{eff} with A agrees, at least in the direction of the trend, with the data of Watson.

Both Watson [7] and Kurzweg and de Zhao [9] have shown theoretically that K_{eff} is proportional to

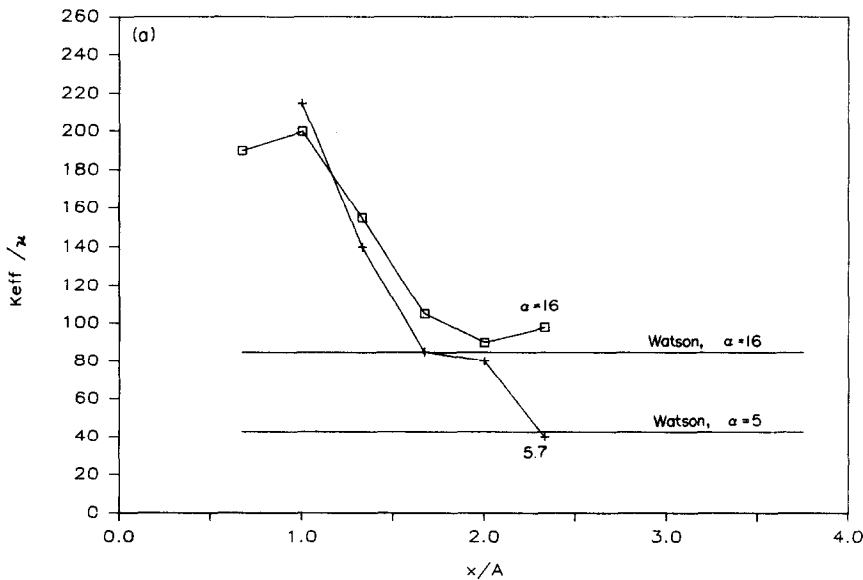


FIG. 8(a). Effective diffusivity for the uniform tube, with $A/d = 3$. Horizontal lines are data of Watson [7].

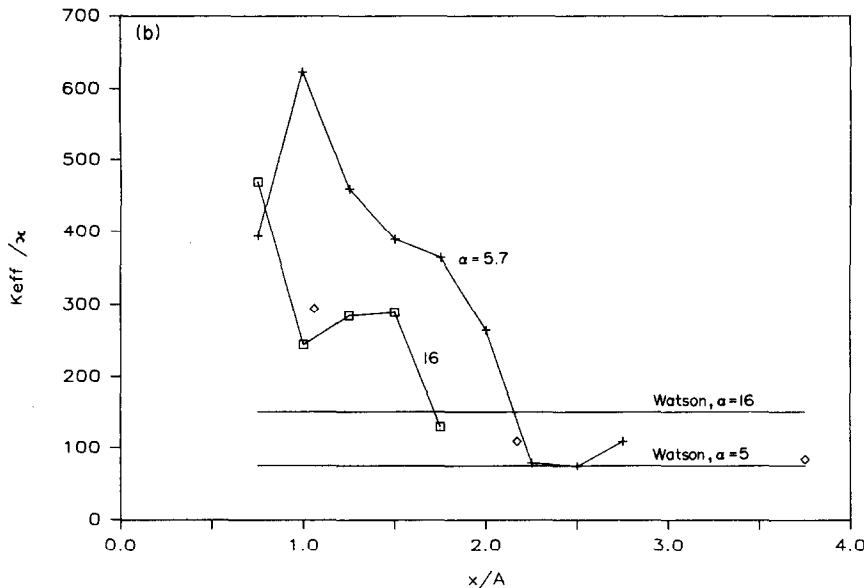


FIG. 8(b). Effective diffusivity, $A/d = 4$. Curves are from the uniform tube; isolated points are from the conical section. Horizontal lines are from Watson [7].

α , in the limit of large α . The results of the present investigation do not support such a result. However, the previous authors assumed a constant time-area averaged axial gradient in the field, whereas this experiment imposes no particular form on $d\langle\bar{T}\rangle/dx$. Here $\langle\bar{T}\rangle$ decreases with distance from the screen, but not with constant slope, which is why the functional dependence of K_{eff} on x does not mirror that of Q_{conv} . In addition, in the experiment there is a net heat loss through the tube walls, whereas the theoretical work assumed impermeable walls as a boundary condition.

5. CONCLUSIONS

To summarize, the present study reveals an instantaneous temperature field the duty cycle of which, but not amplitude, decreases with distance from the heat source. A mean temperature field is found which has a negative radial gradient in the uniform tube, but a complex radial gradient in the conical tube, consistent with steady velocity drift profiles previously reported in refs. [12, 16]. Heat is both lost through, and received from, the test section walls, but the net effect is dissipative, which causes the convective energy transfer, per cycle, to be a decreasing function of distance from the heat source. The effective diffusivity increases with flow amplitude, more strongly at $\alpha = 5.7$ than at $\alpha = 16$, but does not increase by a constant scale factor as α varies from 5.7 to 16. A linear dependence of K_{eff} on α is not observed; therefore existing theories will have to be modified to cover cases for which the boundary conditions do not involve a time-area averaged axial gradient of the field which is constant.

Acknowledgements—The authors would like to thank the National Science Foundation biomechanics program for support of this work. In addition, the authors are very grate-

ful to the late Professor Stanley Corrsin, whose advice and guidance made the work not only possible, but pleasurable as well.

REFERENCES

1. P. P. Lunkenheimer, I. Frank, H. Ising, H. Deller and H. Dickhut, Intrapulmonaler gaswechsel unter simulierter apnoe durch transtrachealen, periodischen intrathorakealen druckwechsel, *Anesthetist* **22**, 232–238 (1972).
2. D. J. Bohn, K. Miyasaka, B. E. Marchak, W. K. Thompson and A. C. Bryan, Ventilation by high-frequency oscillation, *J. Appl. Physiol.: Respirat. Environ. Exercise Physiol.* **48**, 710–716 (1980).
3. A. Slutsky, J. M. Drazen, R. H. Ingram, R. D. Kamm, A. H. Shapiro, J. J. Fredberg, S. H. Loring and J. Lehr, Effective pulmonary ventilation with small volume oscillations at high frequency, *Science* **209**, 609–610 (1980).
4. G. I. Taylor, Diffusion and mass transport in tubes, *Proc. Phys. Soc. B* **67**, 857–869 (1954).
5. R. Aris, On the dispersion of a solute in a fluid flowing through a tube, *Proc. R. Soc. Lond. A* **235**, 67–77 (1955).
6. P. C. Chatwin, On the longitudinal dispersion of passive contaminant in oscillatory flows in tubes, *J. Fluid Mech.* **71**, 513–527 (1975).
7. E. J. Watson, Diffusion in oscillatory pipe flow, *J. Fluid Mech.* **133**, 233–244 (1983).
8. C. H. Joshi, R. D. Kamm, J. M. Drazen and A. S. Slutsky, An experimental study of gas exchange in laminar oscillatory flow, *J. Fluid Mech.* **133**, 245–254 (1983).
9. U. H. Kurzweg and Ling de Zhao, Heat transfer by high-frequency oscillations: a new hydrodynamic technique for achieving large effective thermal conductivities, *Physics Fluids* **27**, 2624–2627 (1984).
10. U. H. Kurzweg, Enhanced heat conduction in fluids subjected to sinusoidal oscillation, *J. Heat Transfer* **107**, 459–462 (1985).
11. U. H. Kurzweg, Temporal and spatial distribution of heat flux in oscillating flow subjected to an axial temperature gradient, *Int. J. Heat Mass Transfer* **29**, 1969–1977 (1986).
12. R. S. Budwig, Two unsteady heat transfer experiments: I. In grid-generated isotropic turbulence; II. In laminar

- oscillatory flow in straight and conical tubes, Ph.D. thesis, Johns Hopkins University (1985).
13. R. A. Peattie, A simple low-drift circuit for measuring temperatures in fluids, *J. Phys. E: Scient. Instrum.* **20**, 565–567 (1987).
 14. J. C. LaRue, T. Deaton and C. H. Gibson, Measurement of high frequency turbulent temperature, *Rev. Scient. Instrum.* **46**, 757–764 (1975).
 15. J. Hojstrup, K. Rasmussen and S. E. Larsen, Dynamic calibration of temperature wires in still air, *DISA Information* **20**, 22–30 (1976).
 16. J. B. Grotberg, Volume-cycled oscillatory flow in a tapered channel, *J. Fluid Mech.* **141**, 249–264 (1984).
 17. J. H. Gerrard, An experimental investigation of pulsating turbulent water flow in a tube, *J. Fluid Mech.* **46**, 43–64 (1971).

TRANSFERT THERMIQUE DANS DES ECOULEMENTS LAMINAIRES OSCILLATOIRES DANS DES TUBES CYLINDRIQUES ET CONIQUES

Résumé—On réalise un écoulement poussé par un piston dans un tube de façon à étudier l'effet de la fréquence sur le transfert d'un contaminant scalaire passif dans un écoulement oscillatoire. Deux géométries de section du tube d'essai sont utilisées: l'une est droite, circulaire et uniforme, l'autre est à réduction uniforme (conique). L'écoulement est conduit à des fréquences de respiration humaine, lente ou normale ou à haute fréquence. Une grille de fils fins et parallèles, à espacement serré, est placée perpendiculairement à l'écoulement dans la section d'essai et elle est chauffée de façon à dissiper une puissance constante dans le fluide. On mesure les champs de température moyens et instantanés en fonction de la position. Les résultats sont cohérents avec les conséquences d'un transport de chaleur par combinaison de convection et de diffusion. Le transport convectif augmente avec la fréquence, à amplitude constante, mais la diffusivité effective ne s'accorde pas avec les conséquences des théories basées sur l'hypothèse d'un gradient moyen axial constant du champ scalaire.

WÄRMEÜBERGANG IN LAMINARER OSZILLIERENDER STRÖMUNG DURCH ZYLINDRISCHE UND KONISCHE ROHRE

Zusammenfassung—Um den Einfluß der Frequenz auf den Transport einer inaktiven ungerichteten Verunreinigung in einer oszillierenden Strömung abzuschätzen, wurde durch einen Kolben eine Rohrströmung erzeugt. Für die Versuche wurden zwei verschiedene Rohrgeometrien benutzt: ein gerades, gleichmäßig rundes Rohr und ein konisches, kontinuierlich verjüngtes Rohr. Die Strömung wurde mit Frequenzen moduliert, wie sie für die menschliche Atmung im Ruhezustand, bei normaler und bei hoher Atemfrequenz typisch sind. In einer Ebene senkrecht zur Strömungsrichtung sind in geringem Abstand dünne, parallele Drähte angeordnet, die durch elektrische Beheizung einen konstanten Wärmestrom an das Fluid abgeben. Die daraus in verschiedenen Abständen resultierenden zeitabhängigen und über die Zeit gemittelten Temperaturfelder werden erfaßt. Die Meßergebnisse stimmen mit dem Ergebnis überein, welches sich durch die Überlagerung des Wärmetransports durch Konvektion und Diffusion ergibt. Es zeigt sich, daß der konvektive Wärmetransport bei konstanter Amplitude mit der Frequenz ansteigt. Das effektive Diffusionsvermögen verhält sich jedoch nicht entsprechend der Theorie, die auf einem im Mittel konstanten, axialen Gradienten des Skalarfeldes basiert.

ТЕПЛОПЕРЕНОС ПРИ ЛАМИНАРНОМ ОСЦИЛЛИРУЮЩЕМ ТЕЧЕНИИ В ЦИЛИНДРИЧЕСКИХ И КОНИЧЕСКИХ ТРУБАХ

Аннотация—Для оценки влияния частоты на перенос пассивной скалярной примеси в осциллирующем потоке при помощи поршней создается течение в трубах. Используются два участка экспериментальных труб: один прямой, круглый и цилиндрический и второй—равномерно сужающийся (т.е. конический). Течение вызывается при частотах, характерных для дыхания человека в состоянии покоя, в нормальных условиях, а также при высокой частоте. На экспериментальном участке перпендикулярно потоку устанавливается экран из близко расположенных параллельных тонких проволок, которые нагреваются так, чтобы рассеивать постоянную мощность в потоке жидкости. Измеряются возникающие усредненные по времени и мгновенные значения температуры полей в зависимости от координат. Показано, что полученные результаты соответствуют теплопереносу, обусловленному совместным действием конвекции и диффузии. Найденно, что конвективный теплоперенос возрастает с увеличением частоты при постоянной амплитуде, однако эффективный коэффициент температуропроводности не подчиняется теоретическим оценкам, основанным на предположении о постоянстве среднего осевого градиента скалярного поля.